ELSEVIER

Fin efficiency of extended surfaces in two-phase flow

Vijayaraghavan Srinivasan* and Ramesh K. Shah†

* Praxair Inc., Tonawanda, New York, and

† Department of Mechanical Engineering, University of Kentucky, Lexington, Kentucky

Compact plate-fin heat exchangers and other extended surface heat exchanges are used in several two-phase flow applications, such as condensation, boiling, or moist-air cooling. Because of simplicity and lack of better information, designers often use fin efficiency formulas for two-phase flows that are derived based on uniform heat transfer coefficient. However, the heat transfer coefficient h on the fin surface under condensation or boiling may vary significantly compared to the single-phase forced convection attributable to the possible existence of different two-phase flow regimes on the fin surface, including the condition of partial dryout. Thus, the use of constant h fin efficiency formulas (of single-phase flow) for two-phase flow situation may result in serious errors. A critical assessment is made in this paper of the various methods available for calculating fin efficiency in practical fin configurations with condensation, moist air cooling, and boiling on the extended surfaces. Conditions under which the use of constant h can be made are identified. Based on the literature review, some specific design recommendations are made for the determination of the fin efficiency for two-phase flow heat exchanger applications.

Introduction

Fins or extended surfaces in heat exchangers are primarily used to increase the surface area and, consequently, to enhance the heat transfer rate. Much literature exists on heat transfer from extended surfaces in single-phase forced convection. The fin efficiency calculation methods derived for such cases are based on a uniform heat transfer coefficient on the fin surface, constant fluid and fin material properties, and a number of other idealizations. A critical assessment of the fin efficiency calculation methods for rectangular fins in single-phase forced convection was done by Huang and Shah (1992). There are, however, many applications where extended surfaces are used in two-phase flow applications. Cryogenic main condensers/reboilers use plate-fin exchangers. Integral finned tubes are commonly used to enhance heat transfer in condensers. Cooling and dehumidification of air is another important area where extended surfaces are extensively employed. Similarly, reboilers use low-finned tubes to enhance heat transfer rate for boiling applications.

The important feature that distinguishes two-phase flow fin analysis from single-phase is that the heat transfer coefficient h on the fin surface may be highly nonuniform and may not be treated as uniform, thus introducing additional complexity in the analysis. For example, in boiling, the variation in h may be of the order of 50–1 or more. It was shown by Haley and Westwater (1965) that stable nucleate, transition, and film boiling can exist simultaneously at adjacent positions on a fin. In such cases, the usefulness of the fin efficiency approach is curtailed.

Similarly, in condensation, heat transfer from the fin surface is tightly coupled to the condensation process on the fin. Variations in condensate film thickness along the fin surface result in nonuniform h. The orientation of the fin with respect to the prime surface also affects the condensation process. Generally, numerical methods have been preferred to solve the system of equations governing the condensation process on extended surfaces.

Cooling and dehumidifying of air is another area where fins are extensively employed to increase surface area. The fin performance is influenced by the combined heat and mass transfer associated with cooling and dehumidification of air. The heat transfer from the fin surface takes place through the simultaneous process of convection and condensation of moisture present in the air. Simplification is achieved in the analysis by assuming a lumped parameter model to account for the mass transfer effects resulting in simplified fin efficiency formulas to predict the overall fin performance. However, numerical methods are used, if any variations in moist air properties along the fin surface are considered.

The objective of this work is to identify principal fin configurations in two-phase flow applications and evaluate different approaches that are used for determining the fin efficiency. Based on the evaluation, appropriate methods for calculating the fin efficiency under different fin orientations are recommended for condensation, boiling, and moist-air cooling. Wherever possible, the range of applicability of each of the methods is identified.

Fin configurations in two-phase flow applications

There are several applications where fins are used in two-phase flow situations. Some of the principal applications are reviewed below.

Address reprint requests to Dr. R. K. Shah, Department of Mechanical Engineering, University of Kentucky, 521 CRMS Bldg., Lexington, KY 40506-0108, USA.

Received 2 April 1996; accepted 1 November 1996

Int. J. Heat and Fluid Flow 18:419–429, 1997

655 Avenue of the Americas, New York, NY 10010

0142-727X/97/$17.00
PII S0142-727X(97)00013-1

Cryogenic plate-fin heat exchangers

Plate-fin heat exchangers are extensively used in cryogenic industries. In a plate-fin heat exchanger, the fins are sandwiched and brazed between partition sheets forming flow passages. The flow passages are oriented vertically in a boiling or a condensing application. The resulting fin configuration is shown in Figure 1a. There are also cases where the finned passages could be oriented horizontally. Because of the high h associated with boiling or condensation, the fin efficiency is generally low in these applications.

Conventional refrigeration condensers

Condensers used in the refrigeration industry employ externally finned tubes (low fin tubes). The fins are radially attached, as shown in Figure 1b. The tube enhance the heat transfer rate attributable to the increased surface area of fins and the improved condensate drainage attributable to surface tension.

Automotive evaporators

A typical construction of an automotive evaporator is shown in Figure 1c. These evaporators use louvered fins. The refrigerant is evaporated inside the passages formed between plates. Moist air is cooled on the outside surface of these plates where louvered fins are attached. The louvers break the boundary layer and enhance heat transfer. The condensation of water vapor over the fin surface and its effect on fin efficiency has been studied extensively in the literature.

Nuclear fuel elements

Longitudinal fins, as shown in Figure 1d, on fuel elements increase the heat transfer area and help in heat removal. This configuration presents very interesting possibilities. For example, the temperature on the surface of the fuel element may be high enough to initiate film boiling; whereas, the fin surface temperature may sustain nucleate boiling. The coexistence of different boiling zones presents a challenge to the conventional fin efficiency concept.

The fin configurations described above can be broadly classified under the following classes of problems:
(1) fin efficiency with film condensation;
(2) fin efficiency with moist air cooling; and
(3) fin efficiency under boiling.

Fin efficiency with condensation

Condensation on the practical fin configurations discussed in the previous section can be divided into the following classes of problems:
(1) a vertical longitudinal fin attached to a pipe or a plate from above (Figure 2a);
(2) a vertical longitudinal fin attached to a pipe or plate from beneath (Figure 2b);

Notation

A	cross-sectional area of fin, m^2
A_f	fin surface area, m^2
A_p	primary surface area, m^2
Bi	Biot number at the fin surface, $h\delta_f/2k_f$, dimensionless
C^*	condensation factor, $[h_{lv}(W_a - W)]/[C_{p,m}(t_a - t)]$, dimensionless
$C_{p,m}$	specific heat of moist air, J/kg K
F_1	fin parameter $[\rho_l(\rho_l - \rho_v)gh_{lv}H^3]/[k_l\mu_l(t_a - t_o)]$, dimensionless
F_2	fin parameter, $(\delta_f k_f)/(2Hk_l)$, dimensionless
G_a	mass flux of air, kg/m^2s
g	gravitational acceleration, m/s^2
H	fin height (projecting from the base), m
H_i	height of fin from the base to the interface between two heat transfer regions, m
h	heat transfer coefficient on the fin surface, W/m^2K
h_w	modified heat transfer coefficient for wet fin surface, W/m^2K
h_{lv}	latent heat of vaporization, J/kg
I_n	nth order modified Bessel function of the first kind
K	fin aspect ratio $2H/\delta_f$, dimensionless
K_n	nth order modified Bessel function of the second kind
k_f	fin thermal conductivity, W/m K
k_l	thermal conductivity of saturated liquid, W/m K
L	fin length (perpendicular to the height H) in the x-direction, m
M	parameters, $MH = (16\sqrt{2}/21)^{1/2}(F_1/F_2^4)^{1/8}$
M^*	fin parameter, $(2hL^2)/(k_f\delta_f)$, dimensionless
m	fin parameter $(2h/k_f\delta_f)^{1/2}$, m^{-1}
m_w	fin parameter, $(2h_w/k_l\delta_c)^{1/2}$, m^{-1}
N	number of heat transfer units, $(2hL)/(G_a s C_{p,m})$, dimensionless
P	fin perimeter, m
Q	heat transferred from the base of a fin, W
r_f	fin tip radius, m
r_t	fin root radius, m
s	fin spacing, m
T	fin temperature, $(t - t_a)/(t_o - t_a)$, dimensionless
T_a^*	air temperature, $(t_a - t_o)/(t_{a,i} - t_o)$, dimensionless
t	fin temperature, K
t_a	ambient fluid temperature, K
$t_{a,i}$	air temperature at inlet, K
t_o	fin base temperature, K
W	humidity ratio of saturated air at t, kg/kg of dry air
W_a	humidity ratio of air at t_a, kg/kg of dry air
$W_{a,i}$	humidity ratio of air at inlet, kg/kg of dry air
W_o	humidity ratio of saturated air at t_o, kg/kg of dry air
W^*	humidity ratio, $(W - W_o)/(W_{a,i} - W_o)$, dimensionless
W_a^*	humidity ratio, $(W_a - W_o)/(W_{a,i} - W_o)$, dimensionless
X	x/L, dimensionless
x	Cartesian coordinate along the fin length, m
Y	y/H, dimensionless
y	Cartesian coordinate along the fin height, m
Z	z/H, dimensionless
Z^*	fin parameters, $(4f_2^4/F_1)(L/H)$, dimensionless
z	Cartesian coordinate along the fin thickness direction, m

Greek

γ	square root of the ratio of heat transfer coefficients in two regions of fin, dimensionless
Δ	δ_c/H, dimensionless
ΔT	temperature difference between fin surface and ambient fluid, K
δ_f	fin thickness, m
δ_c	condensate film thickness, m
ε	relative error in predicted fin efficiency, dimensionless
η_f	fin efficiency, dimensionless
$\eta_{f,w}$	wet fin efficiency, dimensionless
μ_l	dynamic viscosity of saturated liquid, Pa s
ρ_l	density of saturated liquid, kg/m^3
ρ_v	density of saturated vapor, kg/m^3

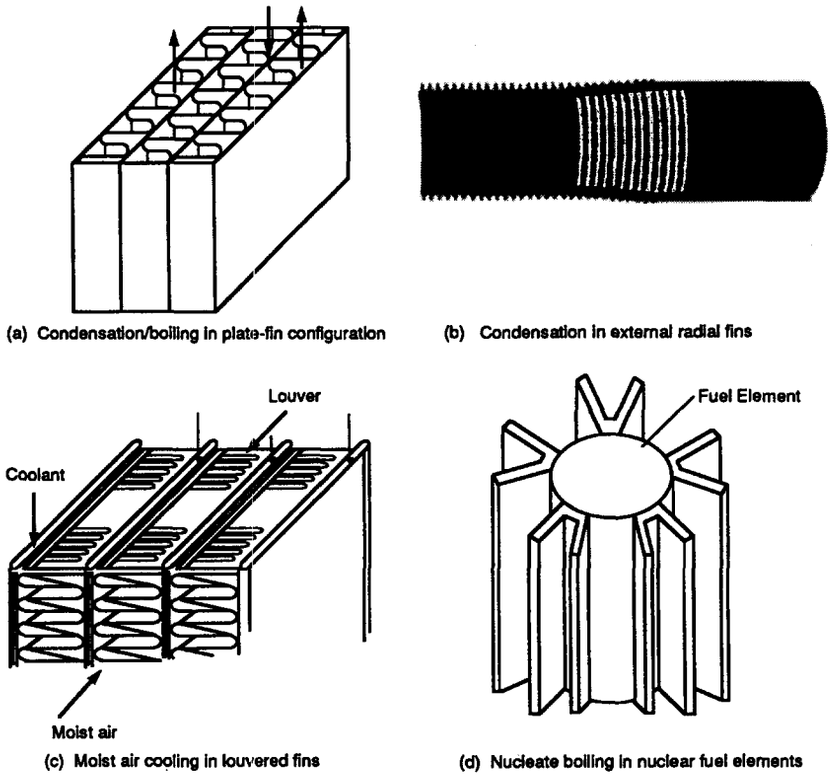

Figure 1 Fin configuration in two-phase flow applications

(3) a vertical longitudinal fin laterally attached to a vertical pipe or a plate (Figure 2c)
(4) a radial fin attached to a horizontal pipe (Figure 2d); and
(5) tubes with internal fins (Figure 2e).

The mathematical formulations of the above five classes of problems differ to some extent from each other. Additional complexities arise if fins are closely spaced so that the condensate films on the neighboring fins interact. Solutions to these problems are obtained as follows.

The derivation of governing equations for fins with condensation generally consists of two steps. In the first step, an equation governing the condensate film thickness and conduction through the film is derived. Usually, Nusselt's hypothesis is invoked (for example, see Patankar and Sparrow 1979) to determine condensate film thickness (and, hence, h). In the second step, conduction through the fin is derived invoking the usual fin idealizations (see Huang and Shah 1992) with the known heat transfer coefficient distribution over the fin from the first step. These two equations are linked and simultaneously solved.

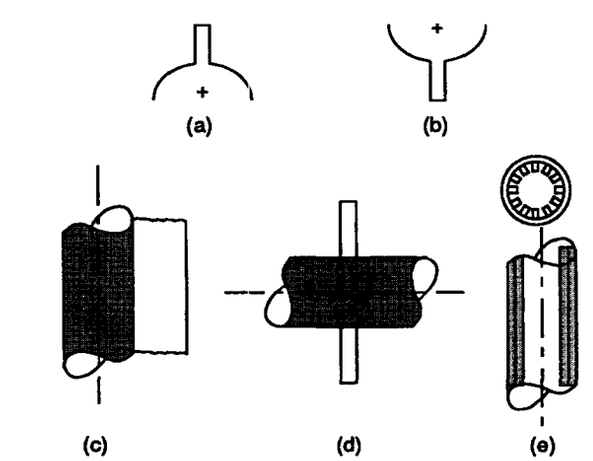

Figure 2 Cross section through fins of different orientations

A vertical longitudinal fin attached to a pipe from above

Consider a thin fin of rectangular cross section having thickness δ_f, width L, and height H. Its root temperature is t_o, and the surrounding vapor temperature is t_a. The fin orientation, as shown in Figure 3 for this particular problem, permits neglecting variations in the fin width or x-direction. This will not be true for the fin of Figure 2c. Neglecting the convective contribution in the film condensation, we get governing equations for the condensate film thickness and the fin temperature (Nader 1978; Burmeister 1982) in dimensionless form as follows.

$$\frac{d\Delta^4}{dZ} = \frac{4T}{F_1} \tag{1}$$

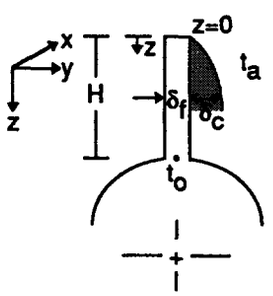

Figure 3 Film condensation on vertical fin facing upward—definition of coordinate axes

and

$$\frac{d^2T}{dZ^2} = \frac{F_1}{3F_2}\Delta^3 \tag{2}$$

with the following boundary conditions:

$$\Delta_{Z=0} = 0 \tag{3}$$

$$T_{Z=1} = 1 \tag{4}$$

$$\left[\frac{dT}{dZ}\right]_{Z=0} = 0 \tag{5}$$

where z has been normalized by the fin height H, $Z = z/H$, dimensionless condensate film thickness $\Delta = \delta_c/H$, and dimensionless fin temperature $T = (t_a - t)/(t_a - t_o)$. The dimensionless fin parameters F_1 and F_2 are defined as follows:

$$F_1 = \frac{\rho_l(\rho_l - \rho_v)gh_{lv}H^3}{k_l\mu_l(t_a - t_o)} \tag{6}$$

$$F_2 = \frac{\delta_f k_f}{2Hk_l} \tag{7}$$

Here, F_1 represents an inverse of the rate of condensation on the fin surface, and F_2 represents a ratio of fin-to-condensate thermal conductivity for a given fin geometry. If F_1 is high, the condensation rate and condensate film thickness on the fin surface are reduced, and therefore, results in higher condensation heat transfer coefficient h (see the relationship between h and F_1 in Equation 13). The increase in h at same values of k_f is equivalent to increasing Biot number ($\mathrm{Bi} = h\delta_f/2k_f$). If we consider a uniform h on the fin surface (equivalent to single-phase convective heat transfer on fins), a higher value of h and the resulting higher Bi number reduces the fin efficiency (Huang and Shah 1992). When $F_2 \to \infty$ (i.e., $k_f \to \infty$), the entire fin approaches the root temperature, and it becomes an ideal fin. It is interesting to note that both Nader (1978) and Burmeister (1982) have observed that the fin efficiency does not depend individually upon F_1 and F_2 but it is a function of F_1/F_2^4, as shown through Equations 8 and 9.

The above set of equations has been solved numerically by Lienhard and Dhir (1974), Nader (1978), and theoretically by Burmeister (1982), to obtain the film thickness Δ and fin efficiency η_f. With some approximations, the theoretical solution presented by Burmeister for the fin efficiency is given by

$$\eta_f = [\tan h(MH)/(MH)]^{6/7} \tag{8}$$

where

$$MH = (16\sqrt{2}/21)^{1/2}(F_1/F_2^4)^{1/8} \tag{9}$$

Here, the fin efficiency is defined as the ratio of actual fin heat transfer to the fin heat transfer that would occur if the entire fin were at the root temperature, and this definition is the same as that for the single-phase heat transfer (Huang and Shah 1992).

Burmeister (1982) also provides a solution for the fin efficiency during condensation assuming an average condensing heat transfer coefficient.

$$\eta_f = \tan h(mH)/mH \tag{10}$$

where

$$m^2 = h_{ave}P/k_f A \tag{11}$$

For a rectangular fin, it reduces to

$$m^2 = 2h_{ave}/k_f\delta_f \tag{12}$$

$$h_{ave} = 2^{3/2}k_l F_1^{1/4}/3H \tag{13}$$

Note that the numerical solution of Lienhard and Dhir (1974) is based on an approximation where a power-law temperature differential (temperature difference between the condensing vapor and fin surface) dependence was assumed with respect to the fin height. This helped eliminate one of the two equations (Equations 1 and 2). They have presented their fin efficiency results as a function of parameter E in graphical form; E is related to the parameters F_1 and F_2 as $E = (1/\sqrt{2})(F_1/F_2^4)^{1/4}$.

The values predicted by Burmeister's (1982) closed-form solutions (Equations 8 and 10) and the solutions of Lienhard and Dhir (1974) are compared with the more accurate numerical solutions of Nadar (1978) in Table 1. These are compared for practical fin designs, where F_1 can vary from 10 to 10^4, and F_1 can range from 10^7 to 10^{13}. For example, for an aluminum fin (of an aspect ratio of K = 10) with condensing refrigerant R113, F_2 is of the order of 100, and F_1 can range from 10^9 to 10^{12} (which depends on the condensation rate). Burmeister's theoretical solution (Equation 8) is within 2.5% of Nader's solution for the entire range of F_1 and F_2. However, the solution represented by Equation 10, which is based on an average condensation coefficient gives values within 3%, if the fin efficiency is greater than about 80% (or $F_1/F_2^4 < 100$). At lower fin efficiencies, deviations as larger as 13.5% are observed. It is found that the approximation introduced by Lienhard and Dhir in their numerical solution has resulted in a significant deviation (up to 25%) from the more accurate numerical solution of Nader.

A vertical longitudinal fin attached to a pipe from beneath

In this case (Figure 2b), the problem formulation is the same as that for the vertical fin pointing upward. Differential Equations 1 and 2 apply to this situation. With the coordinate system of Figure 4, the boundary conditions are as follows:

$$\Delta_{Z=0} = 0 \tag{14}$$

$$T_{Z=0} = 1 \tag{15}$$

$$\left[\frac{dT}{dZ}\right]_{Z=1} = 0 \tag{16}$$

Lienhard and Dhir (1974) numerically solved Equations 1 and 2 along with the boundary conditions of Equations 14–16 using the same approximation described for upward pointing fins, and they have presented fin efficiency results in graphical form. These values read from graphs are presented in Table 2. The fin efficiency obtained from Equation 10 is also shown in Table 2 for comparison. Because both methods are approximate, significant deviations are observed, especially at low fin efficiency values. At fin efficiencies higher than 90% (or $F_1/F_2^4 < 0.01$), both methods predict values within 10% of each other. It should also be noted that an additional idealization on the film thickness is invoked in the above formulation, where it is zero at $Y = 0$. If the fin is attached to a condensing surface, the condensate from that surface draining along the fin surface may affect the film thickness at $Y = 0$ and subsequently increase the film thickness on the fin surface. An increase in the film thickness decreases conden-

Table 1 Comparison of fin efficiency methods for a vertical fin attached to a pipe from above

F_1	F_2	F_1/F_2^4	η_f Nader (1978)	η_f Burmeister (1982)	ε^+ Burmeister (1982)	η_f Eq. 10	ε Eq. 10	η_f *LD*	ε *LD*
1.0×10^{7}	1.0×10^{1}	1.0×10^{3}	0.4603	0.4563	−0.0086	0.4257	−0.0751	0.5835	0.2676
1.0×10^{7}	1.0×10^{2}	1.0×10^{-1}	0.8745	0.8588	−0.0180	0.8541	−0.0233	0.9509	0.0873
1.0×10^{7}	1.0×10^{3}	1.0×10^{-5}	0.9857	0.9831	−0.0026	0.9827	−0.0030	0.9951	0.0096
1.0×10^{7}	1.0×10^{4}	1.0×10^{-9}	0.9988	0.9983	−0.0005	0.9982	−0.0006	0.9995	0.0007
1.0×10^{9}	1.0×10^{1}	1.0×10^{5}	0.2823	0.2820	−0.0010	0.2441	−0.1354	0.3714	0.3156
1.0×10^{9}	1.0×10^{2}	1.0×10^{1}	0.6969	0.6795	−0.0250	0.6645	−0.0465	0.8570	0.2297
1.0×10^{9}	1.0×10^{3}	1.0×10^{-3}	0.9563	0.9489	−0.0077	0.9476	−0.0090	0.9845	0.0295
1.0×10^{9}	1.0×10^{4}	1.0×10^{-7}	0.9955	0.9946	−0.0009	0.9944	−0.0011	0.9984	0.0030
1.0×10^{11}	1.0×10^{1}	1.0×10^{7}	—	0.1722	—	0.1373	—	0.2288	—
1.0×10^{11}	1.0×10^{2}	1.0×10^{3}	0.4603	0.4563	−0.0086	0.4257	−0.0751	0.5835	0.2676
1.0×10^{11}	1.0×10^{3}	1.0×10^{-1}	0.8745	0.8588	−0.0180	0.8541	−0.0233	0.9509	0.0873
1.0×10^{11}	1.0×10^{4}	1.0×10^{-5}	0.9857	0.9831	−0.0026	0.9827	−0.0030	0.9951	0.0096
1.0×10^{13}	1.0×10^{1}	1.0×10^{9}	—	0.1052	—	0.0772	—	—	—
1.0×10^{13}	1.0×10^{2}	1.0×10^{5}	0.2823	0.2820	−0.0010	0.2441	−0.1354	0.3714	0.3156
1.0×10^{13}	1.0×10^{3}	1.0×10^{1}	0.6969	0.6795	−0.0250	0.6645	−0.0465	0.8570	0.2297
1.0×10^{13}	1.0×10^{4}	1.0×10^{-3}	0.9563	0.9489	−0.0077	0.9476	−0.0090	0.9845	0.0295

$^+\varepsilon$ is the relative error compared to the solution of Nader (1978); $\varepsilon=[\eta_f-\eta_f(\text{Nader(1978)})]/\eta_f$
$^\dagger LD=\eta_f$ values read from Figure 9 of Lienhard and Dhir (1974)

sation heat transfer coefficient. The fin efficiency will, therefore, increase.

A vertical longitudinal fin laterally attached to a vertical pipe

This orientation, as shown in Figure 5, is more complex to analyze than the two previous orientations (Figures 3 and 4). The condensate film thickness across the fin length L is assumed constant in the previous two orientations. In this orientation, because the variation in the fin temperature along the y-direction, the film thickness δ_c depends not only upon on the vertical coordinate z, as in previous orientations, but also on the coordinate y. In addition, the fin temperature also depends upon both y and z.

A coupled pair of differential equations is derived for determining temperature distribution T on the fin surface and condensate film thickness δ_c as functions of the coordinates y and z. The problem has been formulated as follows by Patankar and Sparrow (1979).

$$\frac{\partial^2 T}{\partial Y^2}=\frac{T}{F_2\Delta} \tag{17}$$

$$\frac{\partial \Delta^4}{\partial Z}=\frac{4T}{F_1} \tag{18}$$

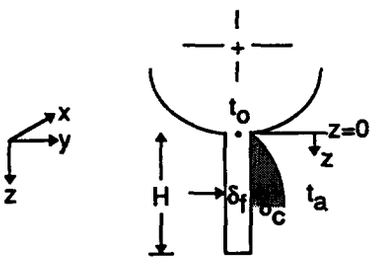

Figure 4 Film condensation on vertical fin facing downward —definition of coordinate axes

The following boundary conditions apply to this problem.

$$T_{Y=0}=1 \tag{19}$$

$$\left[\frac{\partial T}{\partial Y}\right]_{Y=1}=0 \tag{20}$$

$$\Delta_{Z=0}=0 \tag{21}$$

Using a similarity variable $\zeta=y/z^{1/8}$, the system of partial differential equations (Equations 17–18) is transformed to a single dependent variable ζ. A numerical technique was employed to solve the resultant system of transformed equations. Finally, the fin efficiency was obtained as:

$$\eta_f=1.1008\left[\frac{F_2^4}{F_1}\frac{L}{H}\right]^{1/8}=0.9257Z^{*1/8} \tag{22}$$

It should be noted that the similarity solution was found to be accurate in the similarity region for values of $\zeta\le 3.6$. For values of $\zeta>3.6$, Patankar and Sparrow (1979) give results of a numerical solution of Equations 17–21.

Results of the similarity solution for a range of values of F_1 and F_2 along with the more accurate numerical results of Patankar and Sparrow (1979) are presented in Table 2. The fin efficiency obtained by assuming a constant heat transfer coefficient using Equation 10 is also presented in Table 2 for comparison. It is immediately seen that Patankar and Sparrow's results cover a very narrow range of interest. The range of Z^* in their study varies from 0.0001 to 10. Z^* is related to the parameters F_1 and F_2 as $Z^*=(4F_2^4/F_1)(L/H)$. It is a small range considering the exponent in F_2. It is interesting to note that the similarity solution yields results accurate within 2% for $Z^*<0.04$ (or $F_1/F_2^4>100L/H$). A comparison of fin efficiency calculated with an average heat transfer coefficient (Equation 10) shows that its values are within 10% of the more accurate limited numerical results.

A radial fin attached to a horizontal pipe

This orientation is shown in Figure 6. Theoretical models developed for analyzing condensation in these tubes have been pri-

Table 2 Comparison of fin efficiency methods for a vertical fin attached to a pipe from beneath and for a vertical fin laterally attached to a vertical pipe

F_1	F_2	F_1/F_2^4	Z^*	η_f Eq. 10	η_f *LD*	ε *LD*	η_f *PS**	η_f Eq. 22	ε' Eq. 22	ε' Eq. 10
1.0×10^{7}	1.0×10^{1}	1.0×10^{3}	4.0×1.0^{-3}	0.4257	0.608	0.43	0.46	0.4642	0.0091	−0.0746
1.0×10^{7}	1.0×10^{2}	1.0×10^{-1}	4.0×10^{1}	0.8541	0.976	0.14	—	—	—	—
1.0×10^{7}	1.0×10^{3}	1.0×10^{-5}	4.0×10^{5}	0.9827	1.000	0.02	—	—	—	—
1.0×10^{7}	1.0×10^{4}	1.0×10^{-9}	4.0×10^{9}	0.9982	1.000	0.00	—	—	—	—
1.0×10^{9}	1.0×10^{1}	1.0×10^{5}	4.0×10^{-5}	0.2441	0.396	0.62	—	—	—	—
1.0×10^{9}	1.0×10^{2}	1.0×10^{1}	4.0×10^{-1}	0.6645	0.882	0.33	0.70	0.8255	0.1793	−0.0507
1.0×10^{9}	1.0×10^{3}	1.0×10^{-3}	4.0×10^{3}	0.9476	1.000	0.06	—	—	—	—
1.0×10^{9}	1.0×10^{4}	1.0×10^{-7}	4.0×10^{7}	0.9944	1.000	0.01	—	—	—	—
1.0×10^{11}	1.0×10^{1}	1.0×10^{7}	4.0×10^{-7}	0.1373	—	—	—	—	—	—
1.0×10^{11}	1.0×10^{2}	1.0×10^{3}	4.0×10^{-3}	0.4257	0.608	0.43	0.46	0.4652	0.0091	−0.0746
1.0×10^{11}	1.0×10^{3}	1.0×10^{-1}	4.0×10^{1}	0.8541	0.976	0.14	—	—	—	—
1.0×10^{11}	1.0×10^{4}	1.0×10^{-5}	4.0×10^{5}	0.9827	1.000	0.02	—	—	—	—
1.0×10^{13}	1.0×10^{1}	1.0×10^{9}	4.0×10^{-9}	0.0772	—	—	—	—	—	—
1.0×10^{13}	1.0×10^{2}	1.0×10^{5}	4.0×10^{-5}	0.2441	0.396	0.62	—	—	—	—
1.0×10^{13}	1.0×10^{3}	1.0×10^{1}	4.0×10^{-1}	0.6645	0.882	0.33	0.70	0.8255	0.1793	−0.0507
1.0×10^{13}	1.0×10^{4}	1.0×10^{-3}	4.0×10^{3}	0.9476	1.000	0.06	—	—	—	—

ε is the relative error compared to the predictions of Eq. 10; $\varepsilon=[\eta_f-\eta_f\,[\text{Eq. (10)}]/\eta_f]$

ε' is the relative error compared to the numerical predictions of Patankar and Sparrow (1979) $\varepsilon'=[\eta_f-\eta_f[PS^*]]/\eta_f$

* *PS*=numerical solution of Patankar and Sparrow (1979)

† *LD*=η_f values read from Figure 9 of Lienhard and Dhir (1974)

marily based on two principal approaches. The approach used by Beatty and Katz (1948) employs Nusselt's equation for describing condensate drainage from horizontal tube and a vertical surface (fin). Their model assumes that gravity is the dominant force that drains condensate from the condensing surface. The model used by Rudy and Webb (1985), Honda and Nozu (1987), and Karkhu and Borovkov (1971) takes into account the surface tension effect on the behavior of condensate. This effect is composed of two factors. The condensate film thickness is reduced at the upper part of the fin surface, which tends to increase heat transfer. On the lower part of the tube, the surface tension effect tends to retain the condensate between the fins, which tends to decrease heat transfer. Thus, this model divides the heat transfer surface into "unflooded" (upper part) and "flooded" (lower part) regions. Karkhu and Borovkov have shown that surface tension forces have marked effect when We > 10. The Weber number We is calculated by determining the submergence of the fins using equations given by Karkhu and Borovkov (1971) or Webb et al. (1985).

In the gravity-dominated condensation (Beatty and Katz 1948), it is assumed that the condensate is drained from the vertical fins and from the base tube by gravity forces. Thus, Nusselt's equation for horizontal tubes for the tube surface and Nusselt's equation for vertical surface for the fin surface are used to determine the condensation heat transfer coefficient. The fin is assumed to be at its root temperature. The heat transfer on the fin surface is corrected by fin efficiency calculated using the solution given by Gardner (1945) for annular fins (see equation 24).

In surface tension-dominated condensation, several different methods have been used to determine the heat transfer rate. In all these methods, distinction is made between the flooded and unflooded region by calculating the tube region under submergence (flooded region). Thus, the tube and fin surface area in the flooded and unflooded regions are determined. The methods primarily differ in the procedures used for calculating the heat transfer coefficient. The condensate film thickness in the unflooded region is governed by surface tension, and therefore, it is a function of the condensate profile. Idealizations on the shape of the condensate profile lead to different methods of estimating the condensation heat transfer coefficient. The fin surface is assumed to be at the root temperature. The heat transfer rate is corrected by the fin efficiency. In the unflooded region, the fin efficiency is approximated by Webb et al. (1985) as:

$$\eta_f=\frac{\tan h[m(H+\delta_f/2)]}{m(H+\delta_f/2)} \tag{23}$$

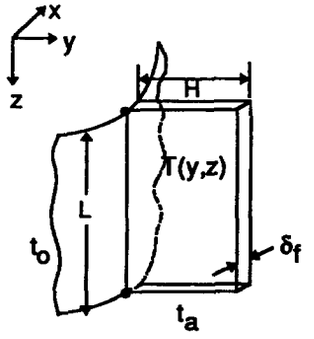

Figure 5 Film condensation on vertical fin laterally attached —definition of coordinate axes

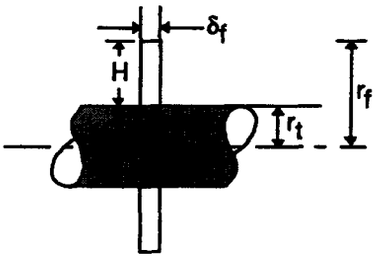

Figure 6 Film condensation on vertical, radial fin attached to a horizontal tube

whereas, Honda and Nozu (1987) use equations for a circular fin with a uniform condensation coefficient on the fin surface given by:

$$\eta_f = \frac{2}{mH(r_f/r_t+1)}\left[\frac{I_1(mr_1)K_1(mr_f) - I_1(mr_f)K_1(mr_t)}{I_o(mr_t)K_1(mr_f) + I_1(mr_f)K_o(mr_t)}\right] \quad (24)$$

In the flooded region, Webb et al. (1985) neglect fin efficiency and Honda and Nozu (1987) obtained the fin efficiency from the solution of radial conduction as:

$$\eta_f = \left[1 + \frac{h}{2\delta_f k_f} ln\left(\frac{r_f}{r_t}\right)\right]^{-1} \quad (25)$$

A comparison of fin efficiency values (for both flooded and unflooded regions) predicted by Equations 23–25 is done for practical fin designs commonly used in condensers with horizontal integral-fin tubes. The results are shown in Table 3, where the fin efficiency η_f is predicted for the following range of fin parameters:

Tube diameter ($2r_t$): 19.0 mm;
Fin height, H: 1.5 to 9.0 mm;
Fin thickness, δ_f: 0.25 mm, 0.5 mm;
Thermal conductivity, k_f: 60 W/m^{2}K (nickel) and
150 W/m^{2}K (aluminum); and
Heat transfer coefficient, h: 100 to 3000 W/m^{2}K.

Note that the low values of heat transfer coefficients in Table 3 are realized in the flooded (condensate bridged) region. The high values correspond to the unflooded region. All methods (Equations 23–25) use a *constant* value of h regardless of a single-phase or two-phase region.

In Table 3, the predictions of Equations 23 and 25 are compared with the more accurate prediction of Equation 24, which is based on the theoretical solution for a radial fin (Gardner

Table 3 Comparison of fin efficiency methods for a radial fin attached to a horizontal fin

H, mm	r_t, mm	h, W/m^{2}K	m, m^{-1}	$m(H+\delta_f/2)$	η_f Eq. 23	η_f Eq. 24	η_f Eq. 25	ε Eq. 23	ε Eq. 25
Case 1: Tube diameter 19 mm; fin thickness=0.5 mm; fin thermal conductivity=150 W/m^{2}K									
3	12.5	100	51.640	0.168	0.991	0.991	1.000	0.000	0.009
9	18.5	100	51.640	0.478	0.930	0.909	1.000	0.023	0.099
3	12.5	500	115.470	0.375	0.956	0.956	0.999	−0.001	0.045
9	18.5	500	115.470	1.068	0.738	0.679	0.998	0.088	0.470
3	12.5	1,000	163.299	0.531	0.916	0.917	0.998	−0.002	0.088
9	18.5	1,000	163.299	1.511	0.600	0.528	0.996	0.137	0.885
3	12.5	3,000	282.843	0.919	0.789	0.792	0.995	−0.003	0.256
9	18.5	3,000	282.843	2.616	0.378	0.309	0.987	0.225	2.198
Case 2: Tube diameter 19 mm; fin thickness=0.25 mm; fin thermal conductivity=150 W/m^{2}K									
3	12.5	100	73.030	0.228	0.983	0.982	1.000	0.001	0.018
9	18.5	100	73.030	0.666	0.874	0.836	0.999	0.046	0.195
3	12.5	500	163.299	0.510	0.921	0.917	0.998	0.005	0.088
9	18.5	500	163.299	1.490	0.606	0.528	0.996	0.148	0.885
3	12.5	1,000	230.940	0.722	0.856	0.849	0.996	0.009	0.174
9	18.5	1,000	230.940	2.107	0.461	0.382	0.991	0.207	1.598
3	12.5	3,000	400.000	1.250	0.679	0.664	0.989	0.021	0.489
9	18.5	3,000	400.000	3.650	0.274	0.212	0.974	0.293	3.602
Case 3: Tube diameter 19 mm; fin thickness=0.5 mm; fin thermal conductivity=60 W/m^{2}K									
3	12.5	100	81.650	0.265	0.977	0.978	1.000	0.000	0.022
9	18.5	100	81.650	0.755	0.845	0.804	0.999	0.051	0.243
3	12.5	500	182.574	0.593	0.897	0.899	0.998	−0.002	0.110
9	18.5	500	182.574	1.689	0.553	0.479	0.994	0.155	1.076
3	12.5	1,000	258.199	0.839	0.817	0.819	0.995	−0.003	0.216
9	18.5	1,000	258.199	2.388	0.412	0.340	0.989	0.211	1.909
3	12.5	3,000	447.214	1.453	0.617	0.618	0.986	−0.001	0.597
9	18.5	3,000	447.214	4.137	0.242	0.187	0.968	0.290	4.166
Case 4: Tube diameter 19 mm; fin thickness=0.25 mm, fin thermal conductivity =60 W/m^{2}K									
3	12.5	100	115.470	0.361	0.959	0.956	0.999	0.002	0.045
9	18.5	100	115.470	1.054	0.743	0.679	0.998	0.095	0.470
3	12.5	500	258.199	0.807	0.828	0.819	0.995	0.011	0.216
9	18.5	500	258.199	2.356	0.417	0.340	0.989	0.226	1.909
3	12.5	1,000	365.148	1.141	0.714	0.701	0.991	0.019	0.414
9	18.5	1,000	365.148	3.332	0.299	0.234	0.978	0.280	3.183
3	12.5	3,000	632.456	1.976	0.487	0.469	0.973	0.038	1.076
9	18.5	3,000	632.456	5.771	0.173	0.129	0.938	0.346	6.280

ε is the relative error compared to the predictions of Eq. 24; $\varepsilon = \{\eta_f - \eta_f\ [\text{Eq. 24}]/\eta_f\}$

1945). Equation 23 used by Webb et al. (1985) predicts fin efficiency that are within 2% of the more accurate prediction of Equation 24 if $m(H + \delta_f/2) \leq 0.4$. This happens at low values of fin height H and heat transfer coefficient h. The use of Equation 23 could result in a larger error (ranging from 3 to 30%) if the calculated fin efficiency is less than 80%. A closer examination of the results shows that the nondimensional parameter $[m(H + \delta_f/2)$ can be used as a rough guideline for the suitability of Equation 23. Thus, Equation 23, which is simple to use, can be employed for both flooded and unflooded regions within 2% accuracy if $m(H + \delta_f/2) \leq 0.4$.

The large deviation between the predictions of Equations 24 and 25 at values of $h > 500$ W/m^{2}K shows that Equation 24 is unsuitable for the unflooded region of the tube, where h normally ranges between 500 W/m^{2}K to 3000 W/m^{2}K. In the flooded (condensate bridged) region, where $h \leq 100$ W/m^{2}K, Equation 25 predicts η_f close to unity. Thus, a fin efficiency of unity in the flooded region is assumed with a small error—less than 1%.

Tubes with internal fins

Internal fins for in-tube condensation is used more as an *augmentation technique* than as an extended surface. In-tube condensers find applications in many air-conditioning and refrigeration systems. Several studies have considered in-tube condensation. Reisbig (1974) used several internally finned tubes for condensation of R-12 and found a minimum increase of about 40% in the condensation heat transfer coefficient (the enhancement of h is referred to unfinned tubes of the same maximum inner radius). Royal and Bergles (1978) studied steam condensation on inside horizontal finned tubes and proposed experimental correlations that take into account the geometric parameters of the finned tube. Similar studies with refrigerants are reported by Luu and Bergles (1979), Said and Azer (1983), and Venkatesh and Azer (1985). All these studies provide correlations to predict the condensation heat transfer coefficient. The proposed correlations use the approach of correcting the plain in-tube condensation heat transfer coefficient correlation by a modifying factor that is a function of the geometrical parameters of the fin. None of the studies presented in the literature use the approach of finding or accounting for the fin efficiency for internally finned tubes.

Fin efficiency with moist air cooling

Two-phase flow situation (partial condensation) on extended surfaces can exist during cooling and dehumidifying of air in an air-conditioning evaporator. When moisture in air condenses on the cooling surface, it results in simultaneous heat and mass transfer. Several studies in the literature have been devoted to analyzing fin efficiency with condensation from moist air.

A typical rectangular fin in a plate-fin type automotive evaporator is shown in Figure 7. The rectangular fin has height H and width L with spacing s and fin thickness δ_f. Moist-air temperature at inlet is $t_{a,i}$. The mass flux of air if G_a. The system of equations that describe moist-air heat transfer on fins in dimensionless form is given by (see McQuiston 1975; Chen 1991) the following:

$$\frac{\partial^2 T^*}{\partial Y^2} + \frac{\partial^2 T^*}{\partial X^2} + M^*(T_a^* - T^*)(1 + C^*) = 0 \tag{26}$$

$$\frac{\partial T_a^*}{\partial X} = -N(T_a^* - T^*) \tag{27}$$

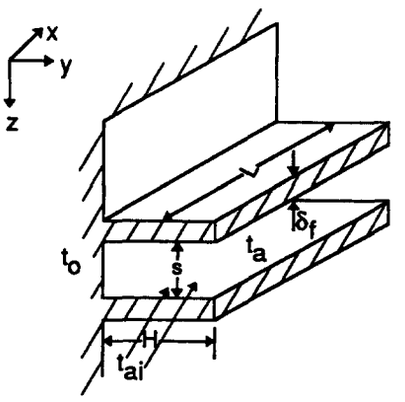

Figure 7 Fin system for moist-air cooling

and

$$\frac{\partial W_a^*}{\partial X} = -N(W_a^* - W^*) \tag{28}$$

with the following boundary conditions:

$$\left(\frac{\partial T^*}{\partial Y}\right)_{Y=1} = 0 \tag{29}$$

$$\left(\frac{\partial T^*}{\partial X}\right)_{X=0} = 0; \qquad (W_a^*)_{X=0} = 1; \qquad (T_a^*)_{X=0} = 1 \tag{30}$$

$$\left(\frac{\partial T^*}{\partial X}\right)_{X=1} = 0 \tag{31}$$

$$T^*_{Y=0} = 0 \tag{32}$$

where $T^* = (t - t_o/(t_{a,i} - t_o)$, $T_a^* = (t_a - t_o)/(t_{a,i} - t_o)$, $Y = y/H$, $X = x/H$, humidity ratio $W^* = (W - W_o)/(W_{a,i} - W_o)$, $W_a^* = (W_a - W_o)/(W_{a,i} - W_o)$, fin parameter $M^* = (2hL^2)/(k_i\delta_f)$ number of heat transfer units $N = (2hL)/(G_a s C_{p,m})$, condensation factor $C^* = (h_{lv}/C_{p,m})[(W_a - W)/t_a - t)]$, and the dimensional variables and parameters are defined in Nomenclature.

The system of equations (Equations 26–32) is reduced to one dimension (1-D) if the environmental conditions are assumed uniform (W and t_a) over the fin length (i.e., the variation in the x-direction is neglected). In this case, the value of N in Equations 27–28 will be zero. Threlkeld (1970) solved the resultant system of equations (1-D) ignoring variations in the x-direction. A uniform condensate film thickness was assumed over the entire fin. By suitably rearranging all the terms and by defining fictitious air enthalpy at different temperatures, Threlkeld had shown that the solution for the dry fin efficiency also applies for the wet fin efficiency, if the heat transfer coefficient for the dry fin is replaced by a modified heat transfer coefficient in which the water film thermal resistance is taken into account. Thus, for a plain rectangular fin of Figure 7, the solution obtained by Threlkeld is given by:

$$\eta_{f,W} = \frac{\tan h(m_W H)}{m_W H} \tag{33}$$

where m_w is defined as:

$$m_W = (h_W/k_l\delta_c)^{1/2} \tag{34}$$

The method described in ARI Standard 410-81 (1972) is based on a 1-D analysis presented by Ware and Hacha (1960). It uses a approach similar to that of Threlkeld (1970). However, the presence of water film and, therefore, its thermal resistance is neglected in the method. The water film temperature is replaced by the surface temperature. The mass transfer potential is computed by assuming that the air adjacent to the fin surface is saturated at the fin surface temperature.

McQuiston (1975) solved the above system of 1-D equations by assuming a linear relationship between the inlet and exit conditions of air on the psychrometric chart. The ratio $(W_a - W)/(t_a - t)$ was assumed constant for the range of air conditions enveloped by the inlet and outlet conditions of the air.

Coney et al. (1989) numerically solved the above system of 1-D equations. However, in their formulation, they related the value of W to t by a second-degree polynominal. Thus, they computed the value of C^* locally along the height of the fin and computed the fin temperature distribution, the condensate film thickness, and fin efficiency as a function of relative humidity of air at inlet. In their model, no variation in the moist-air parameters is considered in the air flow direction.

Chen (1991) performed a rigorous analysis and solved the two-dimensional (2-D) system of equations (Equations 26–32) numerically. The fin temperature distribution and fin efficiency were predicted using their model. Their study showed that streamwise variations in moist air properties have a substantial effect on the fin efficiency, especially at low values of relative humidities.

The 1-D fin efficiency with various values of air relative humidity predicted by the ARI standard (1972), McQuiston (1975) model, and Chen's (1991) model are presented in Figure 8 and compared. The results of Chen's model vary significantly from the predictions of McQuiston's model. This is attributed to the different treatment of the factor C^*. As already pointed out, a constant value of C^* was assumed in the McQuiston model; whereas, Chen based it on a more accurate second-degree polynomial. Because of fin temperature variation along the fin height, the local value of C^* varies over the fin surface. It is seen from Figure 8 that the deviation between the Chen and McQuiston model are more pronounced at low values of relative humidity. The predictions of Chen model compares well with the results of ARI standard.

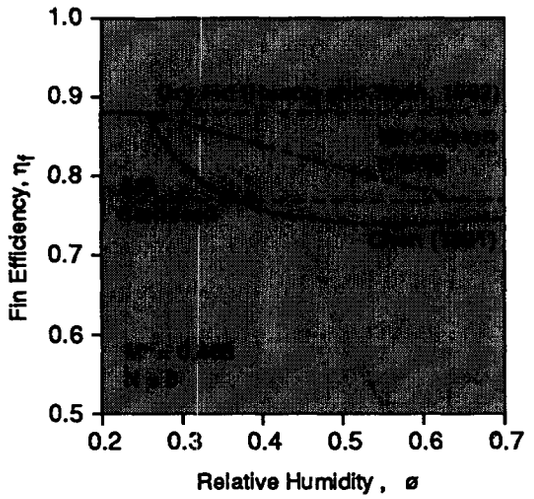

Figure 8 One-dimensional fin efficiency for moist-air flow (from Chen 1991)

Fin efficiency with boiling

Extended surfaces are often used to increase boiling heat transfer to liquids having low hs. Depending on the fin root temperature, nucleate boiling may be initiated at the fin root. This may result in a section of the fin (near the root) cooled by nucleate boiling, and the rest cooled by single-phase convection. If the fin root is at sufficiently high temperature, the entire fin surface may be in nucleate boiling. In some cases, the specified fin root temperature may be such that it results in simultaneous nucleate, transition, and film boiling at adjacent positions on a fin. The individual fin may, thus, be viewed as separate subfins in contact with each other. In other situations, the fin may be wet partially and dry on the rest of the surface. The heat transfer coefficient on the fin surface may vary by as much as 50 to 1 (Cash et al. 1971; Haley and Westwater 1965; Biyikili 1985).

The methods recommended for single-phase heat transfer (Huang and Shah 1992) is obviously not suited for situations where there are such large variations in heat transfer coefficients. The usefulness of variable heat transfer coefficient formulas reported in the literature (for example, Ünal 1985) is also curtailed, because in their formulation the heat transfer coefficient is a function of position along the fin height H rather than a function of temperature difference as would be the case for boiling on a fin.

For a rectangular fin shown in Figure 9 (either vertically or horizontally oriented), the differential equation governing the temperature distribution on the fin is (Lai and Hsu 1967; Hsu 1968; Cumo et al., 1965; Liaw and Yeh 1994a):

$$\frac{d^2T}{dY^2}[m(T)H]^2T \tag{35}$$

with the following boundary conditions:

$$T_{Y=0} = 1 \tag{36}$$

$$\left(\frac{dT}{dY}\right)_{Y=1} = \frac{h(T)T}{k_f H} \tag{37}$$

The conventional idealizations used for the derivation of the temperature profile (Huang and Shah 1992) were applied in obtaining the above Equation 35. It should be noted that $m(T)$ is related to the boiling heat transfer coefficient on the fin surface, and, therefore, it is a function of the difference between the fin surface temperature and the boiling liquid temperature. Here $m(T)$ is defined as:

$$m(T) = [(2h(T)/k_f\delta_f)]^{1/2} \tag{38}$$

The above equation (Equation 35) neglects the radiation effects from fins. The heat transfer coefficient in the boiling section

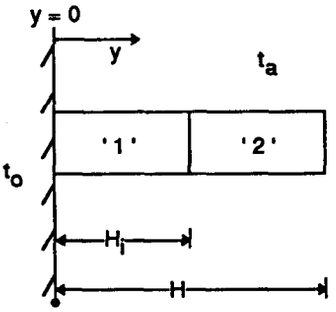

Figure 9 Model for coexistence of two different heat transfer mechanisms on a fin

varies as the temperature difference ΔT to the nth power. It can be expressed as (see Carey 1992):

$$h(T) = C_n \Delta T^n \tag{39}$$

where, C_n is a constant (a function of the saturated property of the fluid). For nucleate boiling, the exponent n takes a value between 2 and 3 (Rohsenow 1962). For film boiling, n takes a value of 0.75. It is interesting to note that for a constant h (single-phase, forced-convection mechanism), n takes a value of zero.

Liaw and Yeh (1994a) studied the thermal characteristics of a single fin, where the heat transfer coefficient was expressed with a power-law-type formula given by Equation 39. In their analysis, the value of the exponent n in Equation 39 was assumed constant. For nucleate boiling, it was taken to be 2. The solution for different values of n was expressed in terms of hypergeometric functions. The temperature distribution and heat transfer rate are given in implicit forms and solved exactly. However, these solutions are valid for the existence of a single heat transfer mechanism on the fin surface, i.e., n is a constant in the solution domain.

As already noted, any fin analysis procedure for boiling must take into account the coexistence of different heat transfer mechanisms at adjacent positions on a fin. The temperature difference between the fin surface and the ambient fluid determines the heat transfer mechanism and local heat transfer coefficient distribution. Thus, one fin can be considered as separate subfins (governed by different heat transfer mechanisms) in contact with each other. The existence of different heat transfer mechanisms complicates the analysis even further. Not only the boundary conditions (Equations 36–37), but the conditions at the interface between the fin regions (that are separated by heat transfer mechanisms) must be specified. Thus, only a numerical solution of Equations 35–37 is possible (Haley and Westwater 1966; Cash et al. 1971; Lai and Hsu 1967; Liaw and Yeh 1994b). These numerical solutions are obtained for different geometries and, therefore are difficult to compare.

It should be noted that fin efficiency is defined as the ratio of the actual heat transfer through the fin to that which would be obtained if the entire fin were at the base temperature. But for boiling, the root (or base) may be at a temperature where film boiling (with a poor heat transfer coefficient) might take place, and at a farther location from the base, the temperature may sustain nucleate boiling (with a higher heat transfer coefficient). The net effect is one of increasing the overall fin heat transfer compared to that based on the temperature potential and local h at the fin base. Thus, the fin efficiency may exceed the value of unity, and, hence, its usefulness in such a situation is curtailed. Therefore, if more than one heat transfer mechanism is coexistent in a fin, the temperature gradient at the fin root rather than the fin efficiency is calculated. The heat transfer rate from the fin is then determined from the temperature gradient at the fin root (see Equation 42).

As shown in Figure 9, for the case of two heat transfer regions on the fin surface (for example, nucleate boiling and single-phase convective heat transfer), where most of the literature cited uses the numerical approach, Lai and Hsu (1967) provide an approximate theoretical solution for the temperature gradient at the fin root. They made an important idealization of a constant boiling heat transfer coefficient h_b and constant convective heat transfer coefficient h_c (i.e., ignoring the variations in h in the boiling region). Alternatively, the method can also be used where transition boiling and nucleate boiling are present. The steps involved in this method are (where nucleate boiling and convective heat transfer are present):

(1) to determine the temperature of incipience of boiling (t_i);
(2) to determine the length of the boiling section (H_i) from (1); and
(3) to calculate the temperature gradient at the fin base $[(\partial t/\partial y)_{y=0}]$.

The temperature of incipience of boiling t_i can be determined experimentally or by using any of the available correlations (see Carey 1992). Lai and Hsu (1967) provide the following equation that relates t_i and H_i

$$\frac{t_i}{t_o} = \frac{1}{\cos h(mH_i)}\left(\frac{1}{1+\gamma \tanh h[\gamma m(H-H_i)]\tan h(mH_i)}\right) \tag{40}$$

Once the value of H_i is obtained from Equation 40, the temperature gradient at the fin base can be obtained using the following expression:

$$\left(\frac{\mathrm{d}t}{\mathrm{d}y}\right)_{y=0} = -mt_o \tan h(mH_i) - \frac{t_i m\gamma \tan h[m\gamma(H-H_i)]}{\cos h(mH_i)} \tag{41}$$

where γ is the square root of the ratio of heat transfer coefficients $[\gamma = (h_1/h_2)^{1/2}]$ in the two regions shown in Figure 9.

It should be noted that the heat transfer rate from the fin is given by:

$$Q = -kA\left(\frac{\mathrm{d}t}{\mathrm{d}y}\right)_{y=0} \tag{42}$$

A comparison of $(\mathrm{d}t/\mathrm{d}y)_{y=0}$ predicted by Equation 41 is made in Figure 10 with the numerical solution of Lai and Hsu (1967) and both numerical and experimental data of Haley and Westwater (1966). The results shown in Figure 10 are for the case of constant saturation temperature of the ambient fluid. Any increase in the fin base temperature t_o increases the length of the nucleate boiling section and consequently reduces the length of the single-phase convective region. Therefore, the assumption of constant h_b introduces increasing error as t_o is increased. However, the deviation between the simplified approach (Equations 41 and 42) and the more detailed numerical results is small for $t_a/t_o \leq 0.5$ in the example illustrated by Lai and Hsu (1967) where the nucleate boiling region is small.

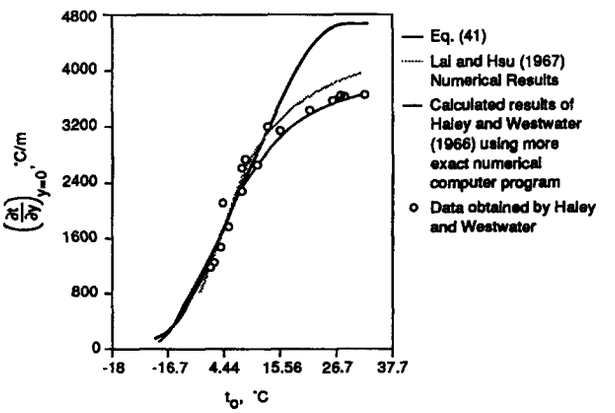

Figure 10 Temperature gradient at base of fin for boiling of freon; H=0.0306 m (from Lai and Hsi 1967)

Conclusions

The methods available for predicting fin efficiency in two-phase flow were assessed. Specifically, two-phase flow situations that occur during condensation of pure vapor, moist-air cooling, and boiling or evaporation in extended surfaces were examined. The following conclusions are reached.

Condensation on fins depends upon on the fin orientation with respect to the prime surface. The parameter F_1/F_2^4 was found to be an important one for the fin efficiency for most of the orientations.

(1) For longitudinal fins that are attached to a pipe from above, Equation 10 can be employed to predict fin efficiency within 3% for $F_1/F_2^4 < 100$ compared to the more accurate numerical methods. However, for larger values of F_1/F_2^4, deviations can be as large as 15%, and a numerical solution is necessary.
(2) For fins that are attached to a pipe from beneath, Equation 10 can be used only for low values of F_1/F_2^4 (less than 0.01). As such for this orientation, there is no accurate numerical solution available as a basis for comparison.
(3) For fins that are laterally attached to a pipe or a vertical surface, Equation 22 can be used within 2% accuracy for values of $Z^* < 0.04$ (or $F_1/F_2^4 > 100L/H$). However, numerical solution may be necessary for $Z^* \geq 0.04$.
(4) For a radial fin attached to a horizontal tube, Equation 24 provides accurate values of fin efficiency. However, if the value of $m(H + \delta_f/2) < 0.4$, Equation 23, which is simpler to use, can be used to predict fin efficiency within 2% accuracy.

For predicting fin efficiency in moist-air cooling, the method of ARI standard (1972) provides a simple approach. However, for applications where a significant variation in the airflow condition (inlet to outlet) can exist, a numerical solution may be necessary.

To predict fin efficiency in boiling, it is first necessary to predict whether there is more than one heat transfer regime active on the fin surface. For situations where two heat transfer mechanisms coexist, Equation 40–42 can be used to predict heat transfer rates through the fin. However, most situations that require describing the boiling coefficient as a function of the temperature difference on the fin surface will require numerical solutions.

References

ARI Standard 410-81, *Forced Circulation Air-Cooling and Air-Heating Coils*. Air Conditioning and Refrigeration Institute, 1972

Beatty, K. O. and Katz, D. L. 1948. Condensation of vapors on outside of finned tubes. *Chem. Eng. Prog.*, **44**, 55–70

Biyikili, S. 1985. Optimum use of longitudinal fins of rectangular profiles in boiling liquids. *J. Heat Transfer*, **107**, 968–970

Burmeister, L. C. 1982. Vertical fin efficiency with film condensation. *J. Heat Transfer*, **104**, 391–393

Carey, V. P. 1992. *Liquid Vapor Phase-Change Phenomena*. Hemisphere, Bristol, PA

Cash, D. R., Klien, G. J. and Westwater, J. W. 1971. Approximate optimum fin design for boiling heat transfer. *J. Heat Transfer*, **93**, 19–24

Chen. L.-T. 1991. Two-dimensional fin efficiency with combined heat and mass transfer between water-wetted fin surface and moving moist airstream. *Int. J. Heat Fluid Flow*, **12**, 71–76

Coney, J. E. R., Sheppard, C. G. W. and El-Shafei, E. A. M. 1989. Fin performance with condensation from humid air: A numerical investigation. *Int. J. Heat Fluid Flow*, **10**, 224–231

Cumo, M., Lopez, S. and Pinchera, G. S. 1965. Numerical calculation of extended surface efficiency. *Chem. Eng. Prog. Symp. Ser.*, **61**, 225–233

Gardner, K. A. 1945. Efficiency of extended surface. *Trans. ASME*, **67**, 621–631

Haley, K. W. and Westwater, J. W. 1965. Heat transfer from a fin to a boiling liquid. *Chem. Eng. Sci.*, **20**, 710–711

Haley, K. W. and Westwater, J. W. 1966. Boiling heat transfer from single fins. *Proc. 3rd Int. Heat Transfer Conf.*, **3**, 245–253

Honda, H. and Nozu, S. 1987. A prediction method for heat transfer during film condensation on horizontal low integral-fin tubes. *J. Heat Transfer*, **109**, 218–225

Hsu, Y. Y. 1968. Analysis of boiling on a fin. NASA TN D-4797, Washington, DC

Huang, L. J. and Shah, R. K. 1992. Assessment of calculation methods for efficiency of straight fins of rectangular profile. *Int. J. Heat Fluid Flow*, **13**, 282–293

Karkhu, V. A. and Borovkov, V. P. 1971. Film condensation of vapor at finely-finned horizontal tubes. *Heat Transfer—Soviet Res.*, **3**, No. 2, 183–190

Lai, F. S. and Hsu, Y. Y. 1967. Temperature distribution in a fin partially cooled by nucleate boiling. *AIChE J.*, **13**, 817–821

Liaw, S. P and Yeh, R. H. 1994a. Fins with temperature-dependent surface heat flux—I. Single heat transfer mode. *Int. J. Heat Mass Transfer*, **37**, 1509–1515

Liaw, S. P. and Yeh, R. H. 1994b. Fins with temperature dependent surface heat flux—II. Multi-boiling heat transfer. *Int. J. Heat Mass Transfer*, **37**, 1517–1524

Lienhard, J. H. and Dhir, V. K. 1974. Laminar film condensation on nonisothermal and arbitrary-heat-flux surfaces and on fins. *J. Heat Transfer*, **96**, 197–203

Luu, M. and Bergles, A. E. 1979. Enhancement of horizontal in-tube condensation of refrigerant—113, *ASHRAE Trans.*, **85**, Pt. 2, 132–145

McQuiston, F. C. 1975. Fin efficiency with combined heat and mass transfer. *ASHRAE Trans.*, **81**, Pt. 1, 350–355

Nader, W. K. 1978. Extended surface heat transfer with condensation —Part I, *Proc. 6th Int. Heat Transfer Conference*, **2**, 407–412

Patankar, S. V. and Sparrow, E. M. 1979. Condensation on an extended surface. *J. Heat Transfer*, **101**, 434–440

Reisbig, R. L. 1974. Condensation heat transfer augmentation inside splined tubes. ASME Paper 74-HT-7

Rohsenow, W. M. 1962. A method of correlating heat transfer data for surface boiling of liquids. *J. Heat Transfer*, **84**, 969–975

Royal, J. H. and Bergles, A. E. 1978. Augmentation of horizontal in-tube condensation by means of twisted-tape inserts and internally finned tubes. *J. Heat Transfer*, **100**, 17–24

Rudy, T. M. and Webb, R. L. 1985. An analytical model to predict condensate retention on horizontal integral-fin tubes. *J. Heat Transfer*, **107**, 361–368

Said, S. and Azer, N. Z. 1983. Heat transfer and pressure drop during condensation inside horizontally finned tubes. *ASHRAE Trans.*, **89**, Pt. 1, 114–134

Threlkeld, J. L. 1970. *Thermal Environmental Engineering*, 2nd Ed., Prentice-Hall, Englewood Cliffs, NJ

Ünal, H. C. 1985. Determination of the temperature distribution in an extended surface with a non-uniform heat transfer coefficient. *Int. J. Heat Mass Transfer*, **28**, 2279–2284

Venkatesh, K. S. and Azer, N. Z. 1985. Enhancement of condensation heat transfer of R-11 by internally finned tubes. *ASHRAE Trans.*, **91**, Pt. 2, 128–144

Ware, C. D. and Hacha, T. H. 1960. Heat transfer from humid air to fin and tube extended surface cooling coils. ASME Paper 60-HT-17

Webb, R. L., Rudy, R. M. and Kedzierski, M. A. 1985. Prediction of the condensation coefficient on horizontal integral-fin tubes. *J. Heat Transfer*, **107**, 368–376